THE JOURNAL OF BIOLOGICAL CHEMISTRY VOL. 292, NO. 3, pp. 1103–1111, January 20, 2017

RFT1 Protein Affects Glycosylphosphatidylinositol (GPI) Anchor Glycosylation*

Received for publication, September 13, 2016, and in revised form, November 17, 2016 Published, JBC Papers in Press, December 7, 2016, DOI 10.1074/jbc.M116.758367

Petra Gottier[‡§], Amaia Gonzalez-Salgado[‡], Anant K. Menon[¶], Yuk-Chien Liu[‖], Alvaro Acosta-Serrano[‖1], and Peter Bütikofer[‡1,2]**

*From the [‡]Institute of Biochemistry and Molecular Medicine and [§]Graduate School of Cellular and Biochemical Sciences, University of Bern, 3012 Bern, Switzerland, the [¶]Department of Biochemistry, Weill Cornell Medical College, New York, New York 10065, and the Departments of [‖]Parasitology and **Vector Biology, Liverpool School of Tropical Medicine, Liverpool L3 5QA, United Kingdom*

Edited by Gerald W. Hart

The membrane protein RFT1 is essential for normal protein *N*-glycosylation, but its precise function is not known. RFT1 was originally proposed to translocate the glycolipid $Man_5GlcNAc_2$-PP-dolichol (needed to synthesize *N*-glycan precursors) across the endoplasmic reticulum membrane, but subsequent studies showed that it does not play a direct role in transport. In contrast to the situation in yeast, RFT1 is not essential for growth of the parasitic protozoan *Trypanosoma brucei*, enabling the study of its function in a null background. We now report that lack of *T. brucei* RFT1 (*Tb*RFT1) not only affects protein *N*-glycosylation but also glycosylphosphatidylinositol (GPI) anchor side-chain modification. Analysis by immunoblotting, metabolic labeling, and mass spectrometry demonstrated that the major GPI-anchored proteins of *T. brucei* procyclic forms have truncated GPI anchor side chains in *Tb*RFT1 null parasites when compared with wild-type cells, a defect that is corrected by expressing a tagged copy of *Tb*RFT1 in the null background. *In vivo* and *in vitro* labeling experiments using radiolabeled GPI precursors showed that GPI underglycosylation was not the result of decreased formation of the GPI precursor lipid or defective galactosylation of GPI intermediates in the endoplasmic reticulum, but rather due to modifications that are expected to occur in the Golgi apparatus. Unexpectedly, immunofluorescence microscopy localized *Tb*RFT1 to both the endoplasmic reticulum and the Golgi, consistent with the proposal that *Tb*RFT1 plays a direct or indirect role in GPI anchor glycosylation in the Golgi apparatus. Our results implicate RFT1 in a wider range of glycosylation processes than previously appreciated.

Trypanosoma brucei is a human and animal parasite endemic in sub-Saharan Africa causing sleeping sickness in humans and nagana in livestock. The life cycle of the extracellular living parasite comprises stages in the midgut and salivary gland of the tsetse fly vector and in the blood of the mammalian host. Alternating between the two organisms, the parasite not only adapts its energy metabolism to the respective environment but also its cell surface protein coat, which is a crucial determinant of the parasite's virulence. Apart from being a deadly pathogen affecting the socio-economic development in endemic areas, the parasite has emerged as an interesting model organism for basic research. Two proliferative stages of *T. brucei*, bloodstream trypomastigotes (bloodstream form parasites) and the insect-stage procyclic trypomastigotes (procyclic form parasites), can easily be cultured *in vitro*. Biological features such as trans-splicing (1), RNA editing (2), and antigenic variation (3) were first described in *Trypanosomatids* and only later also found in other eukaryotes. In addition, *T. brucei* was one of the first organisms in which glycosylphosphatidylinositol (GPI)[3] anchoring of cell surface proteins was described and extensively explored (4, 5). Protein-linked GPI anchors consist of the conserved core structure ethanolamine-HPO_4-Manα1-2Manα1-6Manα1-4GlcNα1-6-*myo*-inositol phospholipid with the amino group of ethanolamine linked to the C terminus of the protein (4, 5). A wide variety of linear and branched glycosyl substituents and additional ethanolamine phosphate moieties can be attached to this core, depending on the protein to which the anchor is attached and the organism in which it is synthesized. The best-studied and most abundant GPI-anchored proteins of *T. brucei* are the variant surface glycoproteins (VSGs) in bloodstream form parasites (6) and the procyclins in procyclic forms (7–9). Although the variant surface glycoprotein GPI core is modified by rather simple galactosyl side chains (5), the GPI anchors of procyclins are the largest and most complex anchors known, comprising large branched *N*-acetyllactosamine (Galβ1-4GlcNAc) and lacto-*N*-biose (Galβ1-3GlcNAc)-containing side chains often capped with α2-3-linked sialic acid residues (10, 11). Based on their C-terminal amino acid sequences containing di- or pentapeptide tandem repeats, procyclins are divided into two classes: EP (rich in Glu-Pro repeats) and

* The work was supported by Swiss National Science Foundation Grants Sinergia CRSII3_141913 and 149353 (to P. B.), National Institutes of Health Grant R21NS093457 (to A. K. M.), and GlycoPar-EU FP7 Marie Curie Initial Training Network Grant GA. 608295 (to A. A. S.). The authors declare that they have no conflicts of interest with the contents of this article. The content is solely the responsibility of the authors and does not necessarily represent the official views of the National Institutes of Health.

[1] Both authors contributed equally to this work.

[2] To whom correspondence should be addressed: Institute of Biochemistry and Molecular Medicine, Bühlstrasse 28, 3012 Bern, Switzerland. Tel.: 41-31-631-4113; E-mail: peter.buetikofer@ibmm.unibe.ch.

[3] The abbreviations used are: GPI, glycosylphosphatidylinositol; VSG, variant surface glycoprotein; mDLO, $Man_9GlcNAc_2$-PP-dolichol; M5-DLO, $Man_5GlcNAc_2$-PP-dolichol; PNGase, protein *N*-glycosidase F; Etn, ethanolamine; Dol, dolichol; Dol-P-Man, dolichol-phosphate mannose; *Tb*RFT1, *Trypanosoma brucei* RFT1; ER, endoplasmic reticulum; GRASP, Golgi reassembly and stacking protein; EMC, endoplasmic reticulum membrane protein complex.

GPEET (rich in Gly-Pro-Glu-Glu-Thr repeats) procyclins (11). Two of the three subclasses of EP procyclins, EP1 and EP3, contain a single *N*-glycosylation site (11, 12), whereas EP2 and GPEET procyclins are not *N*-glycosylated. Interestingly, EP1 and EP3 procyclins are modified exclusively by a triantennary $Man_5GlcNAc_2$ moiety (11), transferred to protein by oligosaccharyltransferase *Tb*STT3B, which is expressed in procyclic forms (13) and specifically uses mature $Man_9GlcNAc_2$-PP-dolichol (mDLO) for transfer to *N*-glycosylation sites (14). Due to the lack of a Golgi α-mannosidase in procyclic form trypanosomes, $Man_9GlcNAc_2$ glycans can only be trimmed to triantennary Man_5-$GlcNAc_2$ that are not further modified (15). Fig. 1*A* shows a schematic representation of a typical *N*-glycosylated EP procyclin.

RFT1 was first described in *Saccharomyces cerevisiae* as a protein "requiring fifty-three," *i.e.* human p53, in a screen of mutants that could be rescued by heterologous expression of p53 (16). Only later, yeast RFT1 (Rft1p) was found to play an essential role in protein *N*-glycosylation (17). The multi-pass transmembrane protein was reported to be localized in the endoplasmic reticulum (ER) of yeast and human cells (17, 18), although no corresponding localization data have been published. The accumulation of the dolichol-linked oligomannose intermediate $Man_5GlcNAc_2$-PP-dolichol (M5-DLO) in *S. cerevisiae* cells depleted of Rft1p but having intact *O*-glycosylation and GPI anchoring suggested that RFT1 is a flippase enabling translocation of M5-DLO across the ER membrane (17). However, this interpretation was challenged by subsequent biochemical studies, where flipping of M5-DLO was assayed *in vitro* using proteoliposomes containing Triton X-100-extracted yeast ER membrane proteins (19, 20). Flipping of M5-DLO occurred robustly in the absence of Rft1p; *e.g.* when proteoliposomes were reconstituted with fractionated ER membrane proteins, M5-DLO translocation activity was found in fractions devoid of Rft1p (19). Similar experiments using sealed microsomes confirmed these findings (21). Hence, it was postulated that *S. cerevisiae* Rft1p has only an indirect involvement in the translocation of M5-DLO (19–21).

More recently, the role of RFT1 was revisited using *T. brucei* as a model organism. By complementation of yeast lacking RFT1 function, *T. brucei* RFT1 (*Tb*RFT1; Tb927.11.11670) was shown to represent a functional homolog of *S. cerevisiae* Rft1p (22). *Tb*RFT1 null procyclic trypanosomes grew nearly normally and had normal steady-state levels of mDLO and reduced but still significant *N*-glycosylation, indicating robust M5-DLO flippase activity. Nevertheless, *Tb*RFT1 null parasites had 30–100-fold greater steady-state levels of M5-DLO when compared with wild-type trypanosomes. Fluorophore-assisted carbohydrate electrophoresis analysis of *N*-glycans released from *N*-linked glycoproteins showed that all *N*-glycans in the *Tb*RFT1 null cells originate from mDLO, indicating that the M5-DLO excess is not used for glycosylation. Together, these results suggested that rather than facilitating M5-DLO flipping, RFT1 appears to promote conversion of M5-DLO to mDLO by another mechanism, possibly by acting as an M5-DLO chaperone (22).

We now report that the lack of *Tb*RFT1 in *T. brucei* procyclic forms not only affects *N*-glycosylation but also GPI anchor glycosylation. In addition, we unexpectedly localize *Tb*RFT1 to both the ER and the Golgi. These results suggest that RFT1 has a pleiotropic influence on protein glycosylation.

Results and Discussion

Procyclins of TbRFT1 Null Cells Exhibit Reduced Apparent Molecular Masses—Based on our previous observation that the lysosomal marker protein p67 is underglycosylated in *Tb*RFT1 null mutants (22), we investigated whether a similar glycosylation phenotype could also be observed for the major surface coat protein of *T. brucei* procyclic forms, EP procyclin. EP procyclins are encoded by three different genes, *EP1–3*, with EP1 and EP3 proteins each containing a single *N*-glycosylation site, whereas EP2 and the other subclass of procyclin, GPEET, are not *N*-glycosylated (11, 23, 24). The relative abundance of EP1–3 and GPEET varies among trypanosome strains and culture conditions (11, 12, 25) and during tsetse infection (26, 27). In the strain used in this study, *T. brucei* Lister 427, GPEET represents the predominant surface protein, but EP is also expressed (25). Analysis by SDS-PAGE and immunoblotting revealed a smaller apparent molecular mass of EP in *Tb*RFT1 null cells when compared with WT trypanosomes (Fig. 1*B*). Treatment of EP from WT cells with protein *N*-glycosidase F (PNGase) to release protein *N*-glycans (Fig. 1*A*) reduced its apparent molecular mass. However, the apparent size of de-*N*-glycosylated EP from WT trypanosomes was larger than that of EP from *Tb*RFT1 null cells, which was unaffected by PNGase treatment (Fig. 1*B*). Together, these results indicate that the altered molecular mass of EP is not only due to altered *N*-glycosylation in *Tb*RFT1 null parasites but involves other modifications caused by lack of *Tb*RFT1.

TbRFT1 Null Procyclins Have Truncated GPI Anchor Side Chains—Because all EP isoforms, as well as GPEET, are GPI-anchored (23, 28), we hypothesized that decreased glycosylation of the GPI anchor side chain may contribute to the observed phenotype. The procyclin GPI anchors are modified by a large heterogeneous, branched side chain comprising poly-*N*-acetyllactosamine and lacto-*N*-biose units that may be capped with sialic acid residues (10, 11) (Fig. 1*A*). Partial or complete loss of this glycan moiety would lead to reduced apparent molecular masses of GPEET and EP. Hence, we analyzed the procyclin GPI anchors by *in vivo* labeling of trypanosomes with [^{3}H]ethanolamine ([^{3}H]Etn), which gets incorporated into the GPI core structure (23, 25). SDS-PAGE and fluorography showed that GPEET, migrating with an apparent molecular mass of 22–29 kDa, was readily labeled with [^{3}H]Etn in WT trypanosomes (Fig. 1*C*). Labeling of GPEET was also observed in *Tb*RFT1 null parasites; however, the protein migrated with a lower molecular mass when compared with WT trypanosomes (Fig. 1*C*). To eliminate molecular mass differences present in the protein part of GPEET, extracts were treated with Pronase, which has been shown to digest the entire protein portion of GPEET down to the C-terminal glycine residue (25). The resulting GPI anchor was again analyzed by SDS-PAGE and fluorography and showed a clear difference in molecular mass between WT and *Tb*RFT1 null parasites (Fig. 1*C*).

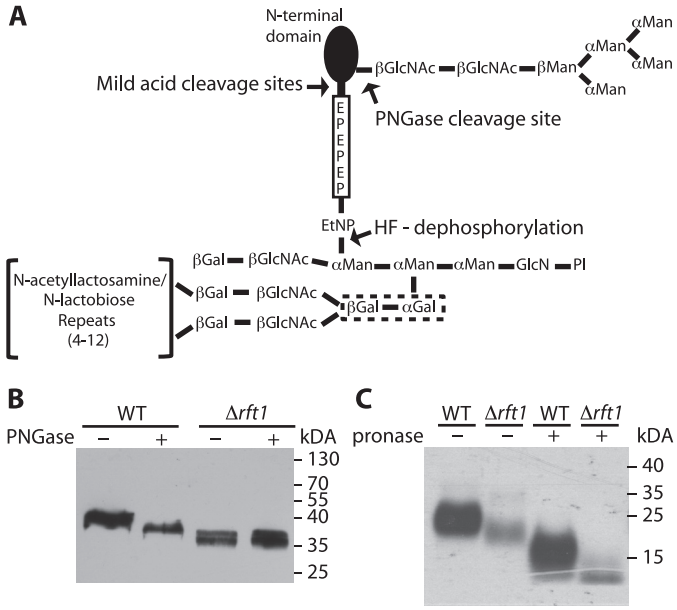

FIGURE 1. **Schematic representation of procyclin glycosylation and analysis of GPI-anchored proteins in *Tb*RFT1 null cells.** *A*, most procyclin isoforms (except EP2 and GPEET) are modified by a homogeneous triantennary $Man_5GlcNAc_2$ glycan near the N terminus. The GPI anchor of all procyclins is modified with several *N*-acetyllactosamine or lacto-*N*-biose repeats, which may be capped with sialic acids depending on the presence of blood sialoglycoconjugates. These repeats are linked to the middle mannose of the GPI anchor core via two consecutive galactose residues (*dotted box*), which are probably added in the ER as suggested in Fig. 2. The C-terminal regions of EP procyclins consist of 22–30 Glu-Pro repeats. *PI*, phosphatidylinositol. *B*, immunoblotting analysis of EP procyclins isolated from WT and *Tb*RFT1 null (Δ*rft1*) cells. Denatured proteins were treated with (+) or without (−) PNGase F to remove *N*-glycans and then separated by SDS-PAGE. After electrotransfer to membranes, EP was visualized by enhanced chemiluminescence using anti-EP antibody and HRP-conjugated anti-mouse IgG. *C*, [^{3}H]ethanolamine labeling and fluorography of GPI-anchored proteins from WT and *Tb*RFT1 null (Δ*rft1*) cells. Trypanosomes were grown in the presence of [^{3}H]ethanolamine, and GPI-anchored proteins were extracted from the delipidated protein pellet using 9% butan-1-ol. Extracts incubated in the absence (−) or presence (+) of Pronase to remove the protein portions of GPEET and EP were separated by SDS-PAGE and analyzed by fluorography.

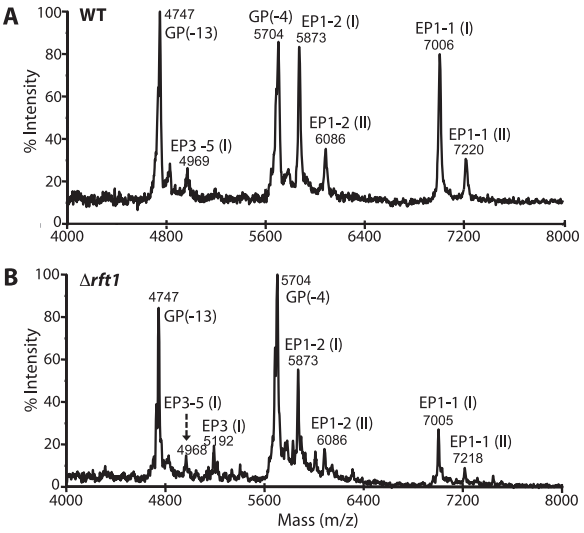

FIGURE 2. **Negative-ion MALDI-TOF-MS analysis of procyclins after removal of the GPI anchors.** *A* and *B*, butan-1-ol extracts from WT (*A*) and Δ*rft1* (*B*) cells were subjected to 48% aqueous hydrofluoric acid dephosphorylation followed by mild trifluoroacetic acid hydrolysis to remove the GPI anchor and generate EP procyclin peptides. The resulting polypeptides, corresponding to the C-terminal portions of procyclins, were analyzed by negative-ion MALDI-TOF-MS. *GP(−4)* and *GP(−13)* refer to GPEET fragments lacking 4 and 13, respectively, amino acids at the N terminus. EP isoforms *EP1-1 (I)* (P(EP)nG-Etn) and *EP1-1 (II)* (PDP(EP)nG-Etn) represent C-terminal mild acid fragments (12). *EP3-5* is an unusual form containing 21 EP repeats (49).

To confirm that the GPEET polypeptide itself is not truncated in *Tb*RFT1 null parasites, its mass was analyzed by MALDI-TOF-MS after sequential treatment with aqueous hydrofluoric acid (to remove the GPI anchor, leaving ethanolamine attached to the C-terminal amino acid (Fig. 1*A*)) and mild trifluoroacetic acid (to cleave Asp-Pro bonds within the EP sequence (Fig. 1*A*)) (12). The results in Fig. 2, *A* and *B*, show that both WT and Δ*Tbrft1* cells express the same GPEET fragments GP-4 and GP-13, representing proteins lacking 4 and 13, respectively, *N*-terminal amino acids. Furthermore, the masses are consistent with the presence of ethanolamine linked to Gly, further corroborating that Δ*Tbrft1* cells are not defective in the transfer of GPIs to proteins. In addition, a series of EP procyclin C-terminal fragments was also detected.

To determine the degree of GPI underglycosylation in Δ*Tbrft1* cells, butan-1-ol extracts (rich in procyclins) were analyzed by GC-MS. As expected, although the WT sample yielded a composition of Man:Gal:GlcNAc:Sia of 1.0:1.4:0.4:0.2, Δ*Tbrft1* cells showed an ~7-fold reduction in the overall GPI sugar content, resulting in a ratio of Man:Gal:GlcNAc:Sia of 1.0:0.2:0.1:~0 (Sia were not detectable). A similar reduction in the overall sugar composition of another Δ*Tbrft1* mutant (*i.e.* B1 cells (22)) was also observed by GC-MS (not shown). Collectively, these results show that trypanosomes lacking *Tb*RFT1 express procyclins with truncated GPI anchor side chains containing fewer poly-*N*-acetyllactosamine/lacto-*N*-biose repeats and sialic acids, thus explaining the observed reductions in apparent molecular masses after SDS-PAGE.

Procyclin GPI Anchor Size Is Restored by Ectopically Expressed TbRFT1—To study whether the observed differences in EP and GPEET molecular masses between WT and *Tb*RFT1 null mutants are indeed due to the lack of *Tb*RFT1, we generated add-back mutants by expressing HA-tagged or untagged copies of *Tb*RFT1 in the Δ*Tbrft1* background. If functional, these ectopically expressed proteins are expected to restore the molecular masses of EP and GPEET to wild-type sizes. Immunoblotting using antibodies against the HA epitope demonstrated that RFT1-HA was expressed in the respective clones (Fig. 3*A*). In addition, the results showed that in *Tb*RFT1 null parasites expressing HA-*Tb*RFT1 or untagged *Tb*RFT1, the apparent molecular mass of EP was comparable with wild-type EP procyclin (Fig. 3*B*), indicating that both tagged and untagged *Tb*RFT1 are functional and restored EP glycosylation as well as GPI glycan maturation. A similar result was obtained by analyzing [^{3}H]Etn-labeled EP and GPEET using SDS-PAGE and fluorography (Fig. 3*C*).

GPI Precursor Synthesis and in Vitro GPI Galactosylation Are TbRFT1-independent—To study whether the lack of *Tb*RFT1 affects the formation of PP1, the GPI precursor added to protein in the ER (29), trypanosomes were cultured in the presence of [^{3}H]Etn, which becomes incorporated into all ethanolamine-capped GPI precursors. Analysis of extracts from WT, *Tb*RFT1 null, and *Tb*RFT1 addback parasites by TLC revealed that PP1

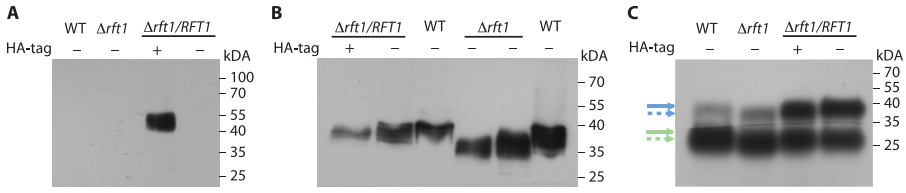

FIGURE 3. **Ectopic expression of *Tb*RFT1 and *Tb*RFT1-HA.** EP and/or GPEET from WT cells, *Tb*RFT1 null cells (Δ*rft1*), and *Tb*RFT1 null cells expressing a HA-tagged (+) or untagged (−) ectopic copy of *Tb*RFT1 (Δ*rft1/RFT1*) were analyzed by SDS-PAGE and immunoblotting. *A* and *B*, enhanced chemiluminescence was used to visualize HA (*A*) or EP (*B*) using corresponding first and secondary antibodies. *C*, EP and GPEET in WT, *Tb*RFT1 null cells (Δ*rft1*), and *Tb*RFT1 null cells expressing a HA-tagged (+) or untagged (−) ectopic copy of *Tb*RFT1 (Δ*rft1/RFT1*) were labeled with [^{3}H]ethanolamine, extracted, and analyzed as described in the legend for Fig. 1. The sizes of wild-type (*solid lines*) and mutant (*dashed lines*) proteins are marked (*blue*, EP; *green*, GPEET).

was the major [^{3}H]Etn-labeled lipid irrespective of the presence or absence of *Tb*RFT1 (Fig. 4*A*).

Assembly of the GPI core structure and attachment to protein occurs in the ER (30–32). At present, it is unclear whether the glycan modification at the central mannose residue starts before or after GPI attachment to protein in the ER, or on protein-bound GPI anchors in the Golgi. It is known that galactose is added *in vitro* to GPI anchor precursors in bloodstream form *T. brucei* (33), suggesting the presence of ER-resident galactosyltransferases that are able to act on GPI precursors. To date, only two *T. brucei* glycosyltransferases involved in GPI processing are known: GT8 and GT3. However, both seem to localize to the Golgi, with GT8 mediating the transfer of the first GlcNAc moiety to the terminal digalactose moiety of the immature GPI anchor (34, 35) and GT3 attaching a galactose residue to GlcNAc (36). To study whether decreased galactosylation in the ER may cause underglycosylation of the GPI anchors in *Tb*RFT1 null cells, we pulse-labeled crude membrane preparations from *Tb*RFT1 add-back and *Tb*RFT1 null parasites with [^{3}H]GDP-mannose ([^{3}H]GDP-Man) in the presence of UDP-GlcNAc and chased the labeled GPI precursors with non-radiolabeled GDP-Man and UDP-Gal. Tunicamycin was added to the assays to inhibit formation of the *N*-glycan precursor dolichyl-pyrophosphate GlcNAc (Dol-PP-GlcNAc). TLC analysis of ^{3}H-labeled GPI lipids after extraction with chloroform/methanol/water followed by butan-1-ol-water partitioning showed that additional more polar species were formed during the chase with UDP-Gal (Fig. 4*B*, *green arrows*). However, we observed no differences in the galactosylation pattern between wild-type and *Tb*RFT1 null cells, indicating that galactosylation of GPI precursors in the ER is not affected by lack of *Tb*RFT1.

The ER lumenal mannose donor dolichol-phosphate mannose (Dol-P-Man) is one of the most prominent radiolabeled lipid species after pulse labeling membranes with [^{3}H]GDP-Man (Fig. 4*B*). As expected, Dol-P-Man as well as the early GPI intermediate Manα1–4GlcNα1–6-myo-inositol phospholipid (Man_1-GlcN-PI) almost completely disappeared during the chase. Interestingly, extracts from both pulse-labeled and chase-labeled Δ*Tbrft1* membranes contained additional polar mannose-containing lipids (Fig. 4*B*, *blue arrows*). A comparison with extracts from membranes labeled in the absence of tunicamycin (Fig. 4*C*) shows that compounds with similar R_f values are also formed by WT membranes as long as *N*-glycan synthesis is enabled. Treatment of the labeled lipids with mild acid led to degradation of Dol-P-Man as well as the unknown polar species from both wild-type and mutant extracts (Fig. 4, *C* and *D*). Conversely, the acid-sensitive lipids were not cleaved by the GPI-specific phospholipase D, whereas the known GPI intermediates were readily hydrolyzed (Fig. 4*D*). Together, these results suggest that the unknown species made by mutant membranes are tunicamycin-insensitive dolichol-linked oligomannose species that most likely originate from a pool of preformed (early) intermediates. We conclude that side-chain glycosylation of newly synthesized GPI precursors occurs normally in Δ*Tbrft1* membranes.

Possible Roles of TbRft1 in GPI Anchor Modification—The defects in GPI anchor maturation of *Tb*RFT1 null cells can be interpreted in two ways. *Tb*RFT1 may have a direct role in GPI anchor glycan modification that is independent of its function in *N*-glycosylation. Alternatively, the defect may result from incomplete *N*-glycosylation of a glycosyltransferase involved in GPI anchor modification, leading to decreased activity and thus incomplete glycan modification.

First, we considered the possibility that the appearance of truncated GPI anchors may be caused by a glycosylation defect occurring in the Golgi. To study whether *Tb*RFT1 is present exclusively in the ER, as suggested for yeast (17), we analyzed the localization of the functional HA-tagged copy of *Tb*RFT1 in the *Tb*RFT1 null background using immunofluorescence microscopy. Co-staining of *Tb*RFT1-HA with an antibody against the ER lumenal chaperone BiP confirmed the expected localization of *Tb*RFT1 in the ER, where it was predominantly found in the perinuclear region (Fig. 5*A*). Interestingly, however, co-staining of *Tb*RFT1-HA with an antibody against the Golgi resident protein *Tb*GRASP (37) also showed co-localization (Fig. 5*A*). In >70% of parasites examined ($n > 100$), *Tb*RFT1-HA co-stained with a spot located between the nucleus and the kinetoplast and representing the Golgi. To exclude the possibility that the observed co-localization of *Tb*RFT1 with *Tb*GRASP is unspecific, we analyzed the localization of an HA-tagged membrane-bound member of the EMC family of proteins, *Tb*EMC3 (Tb927.10.4760), which has been shown in yeast to localize to the ER (38). The results showed <35% co-localization of *Tb*EMC3-HA with *Tb*GRASP (Fig. 5*B*). Although we cannot completely exclude the possibility that a portion of *Tb*RFT1 is localized to the Golgi as a result of saturation of the retention system for ER membrane proteins, we consider it unlikely for the following reasons. (i) *Tb*RFT1-HA shows a similar dual localization when expressed by a different, tetracycline-inducible expression vector in *T. brucei* 427 wild-type cells (Fig. 5*C*); (ii) overexpression of another ER-localized membrane protein, *Tb*EPT (*T. brucei* ethanolamine phosphotransferase), using the same tetracycline-inducible vector showed no Golgi localization and was

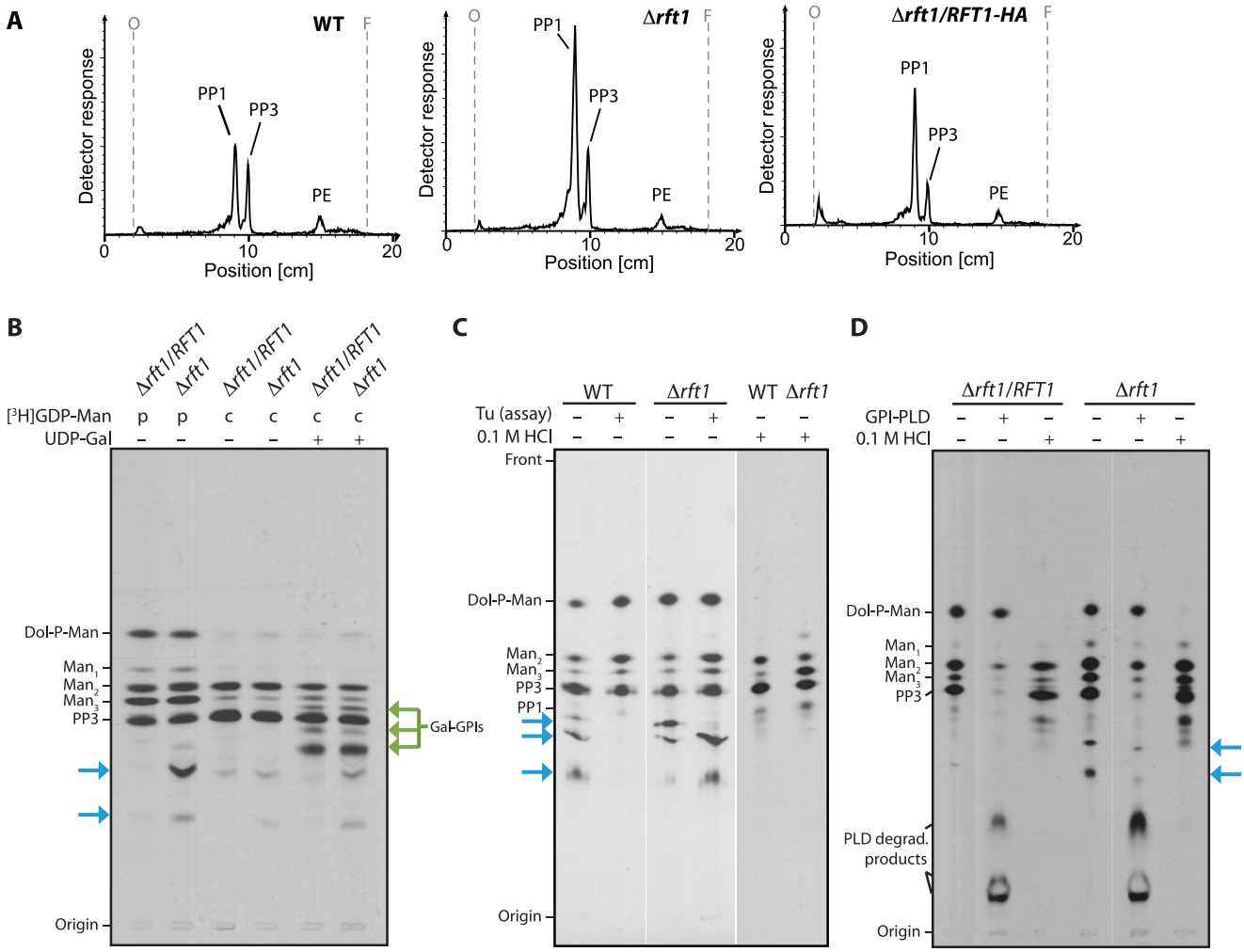

FIGURE 4. **Analysis of GPI precursor formation.** *A*, analysis of *in vivo* [^{3}H]Etn-labeled GPI precursors PP3 and PP1 extracted from WT, *Tb*RFT1 knock-out (Δ*rft1*), and addback (Δ*rft1/RFT1*) cells. Trypanosome densities were adjusted before the addition of [^{3}H]Etn to the cultures. After 4 h of labeling, GPI precursors were extracted, separated by TLC, and visualized using a radioactivity TLC scanner. The migration of PP1, PP3 (50), and phosphatidylethanolamine (*PE*) is indicated. *B–D*, *in vitro* [^{3}H]GDP-mannose (GDP-Man) labeling of GPI precursors. *B*, membranes from hypotonically lysed *Tb*RFT1 knock-out (Δ*rft1*) and addback (Δ*rft1/RFT1*) cells were pulse-labeled (*p*) with [^{3}H]GDP-Man, followed by a chase (*c*) with non-radioactive GDP-Man in the presence (+) or absence of (−) UDP-galactose. ^{3}H-labeled glycolipids were extracted, separated by TLC, and visualized by fluorography. Galactosylated GPI intermediates are indicated with *green arrows*. *Blue arrows* indicate the additional [^{3}H]GDP-mannose-containing species formed in Δ*rft1* extracts. *C*, analysis of ^{3}H-labeled glycolipids from wild-type and Δ*rft1* after a 30-min labeling with [^{3}H]GDP-Man in the presence (+) or absence (−) of tunicamycin (*Tu*) (*lanes 1–4*). *Lanes 5* and *6* show aliquots labeled in absence of tunicamycin that were treated with 0.1 M HCl before TLC. *D*, biochemical analysis of ^{3}H-labeled glycolipids from Δ*rft1* and Δ*rft1/RFT1* after a 30-min labeling with [^{3}H]GDP-Man in the presence (+) of tunicamycin. Primary lipid extracts were split and treated with GPI-specific phospholipase D (*GPI-PLD*) or 0.1 M HCl as indicated. Lipids were re-extracted after treatment and separated by TLC along with an aliquot of untreated primary extract.

specifically targeted to the perinuclear ER (39); and (iii) there is no precedent in trypanosomes for mislocalization of ER proteins on overexpression of a single ER resident. Dual localization of trypanosome proteins in both the ER and the Golgi is not unique to *Tb*RFT1 but has been reported before (40). In contrast, no co-localization was observed between *Tb*RFT1-HA and cathepsin L, a marker for the *T. brucei* lysosome (41) that also localizes between the nucleus and the kinetoplast (Fig. 5*D*). The role of *Tb*RFT1 in glycosylation in the Golgi remains speculative. In a recent publication, RNAi-mediated silencing of the nucleotide sugar transporter *Tb*NST4 responsible for import of UDP-GlcNAc, GDP-mannose, and UDP-GalNAc into the Golgi resulted in production of underglycosylated EP procyclin in *T. brucei* procyclic forms (42). In addition, defective forms of GT3 (36) or GT8 (35, 43) resulted in impaired GPI glycan maturation and reduced protein *N*-glycosylation. It is possible that a lack of *Tb*RFT1 affects Golgi resident proteins involved in glycosylation, by directly interacting with these proteins or by affecting their glycosylation status.

To study the second possibility, we analyzed GPEET procyclin in cells grown in the presence of tunicamycin during 10 days to inhibit *N*-linked glycosylation. The results show that the molecular mass of GPEET was reduced by tunicamycin treatment to that of GPEET in Δ*Tbrft1* cells (Fig. 6*A*). Binding of FITC-labeled concanavalin A to parasites followed by analysis by FACS demonstrated that tunicamycin effectively inhibited *N*-glycosylation (Fig. 6*B*).

Concluding Remarks—We report several new findings that implicate RFT1 in a wider range of glycosylation processes than previously demonstrated. Procyclic form trypanosomes lacking *Tb*RFT1 not only have decreased protein *N*-glycosylation but also produce underglycosylated GPI anchors. The defect is not

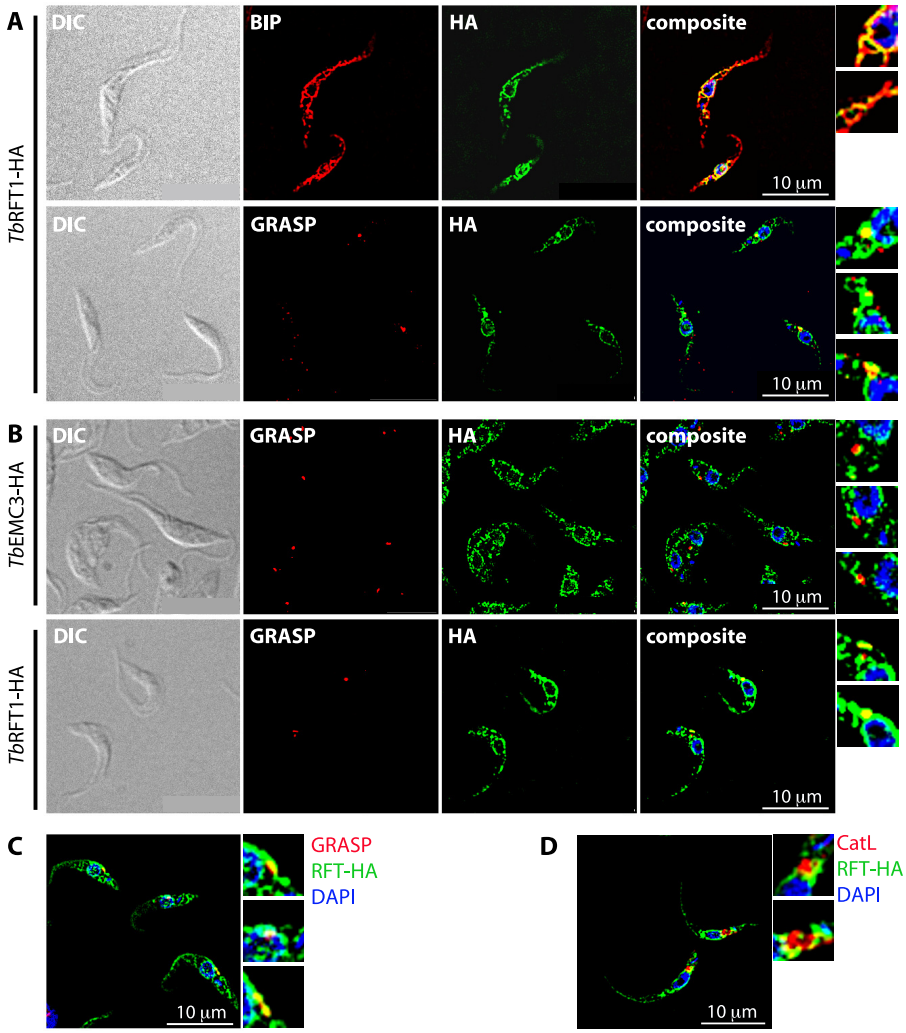

FIGURE 5. **Localization of *Tb*RFT1 in procyclic form parasites.** *A*, functional *Tb*RFT1-HA was co-stained with the ER marker protein BIP (*upper panels*) or the Golgi marker *Tb*GRASP (*lower panels*). The merged channels (composite) show overlap (*yellow color*) of the BIP and *Tb*RFT1-HA signals mainly in the perinuclear zone, with some weaker signal distributed throughout the rest of the cells. Co-staining with the Golgi marker *Tb*GRASP shows that the brightest spots of the HA signal co-localize with the Golgi signal. Some areas were zoomed for better visibility (panels on the *right*). *DIC*, differential interference contrast. *B*, trypanosomes expressing *Tb*EMC3-HA were co-stained with *Tb*GRASP (*upper panels*). The merged channels (composite) show little overlap (*yellow color*) of the signals. Golgi-stained areas were zoomed for better visibility (panels on the *right*). The *lower panels* show co-staining of *Tb*RFT1-HA with *Tb*GRASP done in parallel with the staining shown in the upper panels. Again, *Tb*RFT1 co-localized with *Tb*GRASP. DNA was stained with DAPI (*blue*). *C*, co-staining of *Tb*RFT1-HA (*RFT-HA*) with the Golgi marker *Tb*GRASP in cells transiently expressing *Tb*RFT1-HA under the control of a tetracycline operator. Tetracycline (1 μg/ml) was added to the growth medium for 20 h prior to preparation of slides. *D*, functional *Tb*RFT1-HA was co-stained with the lysosomal marker protein cathepsin L (*CatL*) and DAPI as indicated. The composite shows little overlap (*yellow color*) of the signals. Cathepsin L-stained areas were zoomed for better visibility (panels on the *right*).

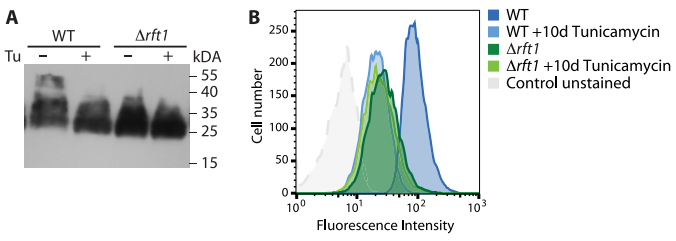

FIGURE 6. **Tunicamycin-mediated inhibition of *N*-glycosylation *in vivo*.** Cells were grown in the presence (+) or absence (−) of 1 μg/ml tunicamycin (*Tu*) during 10 days. *A*, proteins extracted from 2×10^7 cells were separated by SDS-PAGE, and GPEET procyclin was detected by immunoblotting using anti-GPEET antibody 5H3. *B*, cell surface *N*-glycosylation levels were assessed by lectin binding and flow cytometry using FITC-conjugated concanavalin A. The shift in cell surface fluorescence intensity reflects inhibition of *N*-glycosylation by tunicamycin.

associated with the synthesis of the anchor but with GPI processing/maturation steps that likely occur in the Golgi apparatus. A role for *Tb*RFT1 in the Golgi would be consistent with our observation that *Tb*RFT1-HA is dually localized in the ER and Golgi. Our observations open new questions regarding the enigmatic function of *Tb*RFT1 and its orthologs in yeast and mammalian cells.

Experimental Procedures

Materials—Unless otherwise stated, all reagents were of analytical grade and purchased from Sigma-Aldrich (Buchs, Switzerland) or Merck (Darmstadt, Germany). Restriction enzymes were from Fermentas (St. Leon-Rot, Germany), and antibiotics were from Sigma-Aldrich, InvivoGen (Nunningen, Switzer-

land), or Invitrogen (Basel, Switzerland). [1-^{3}H]Etn (40–60 Ci/mmol) and [^{3}H]GDP-Man were from American Radiolabeled Chemicals Inc. (St. Louis, MO). BioMax MS and MXBE films were from GE Healthcare (Buckinghamshire, UK) or Carestream Health (Rochester, NY).

Trypanosome Cultures—*T. brucei* strain Lister 427 procyclic forms were cultured at 27 °C in SDM-79 containing 5% heat-inactivated fetal bovine serum. *Tb*RFT1 knock-out trypanosomes (Δ*Tbrft1*, *Tb*RFT1 null) (22) were grown under the same conditions, but in the presence of 1 μg/ml G418 for the single allele knock-out and an additional 10 μg/ml blasticidin for the double allele knock-out clones. *Tb*RFT1 addback mutants in Δ*Tbrft1* double allele knock-out cells were selected and grown in the same medium, with an additional 2 μg/ml puromycin. *T. brucei* strain Lister 427 29-13 (*TetR T7RNAP*) procyclic forms for tetracycline-inducible gene expression were cultured at 27 °C in SDM-79 containing 10% heat-inactivated fetal bovine serum, 25 μg/ml hygromycin, and 15 μg/ml G418.

Generation of T. brucei RFT1 Addback Procyclic Forms—The generation of the *T. brucei* strain Lister 427 procyclic form *Tb*RFT1 null cell line Δ*Tbrft1::NEO*/Δ*Tbrft1::BLAST* has been described previously (22). For the generation of procyclic trypanosomes constitutively expressing *Tb*RFT1 or 2× HA-tagged *Tb*RFT1 (*Tb*RFT1-HA) in the Δ*Tbrft1* background (Δ*Tbrft1/RFT1* and Δ*Tbrft1/RFT1-HA*), the ORF of *TbRFT1* (Tb927.11.11670) was PCR-amplified with primers TbRFT1β_fwd (tgtagcaagcttgaattcatggacttcaaacgacagctg) and TbRFT1β_rev (ccccgcagatctctactcgccgcttctttttga) or TbRFT1_fwd and TbRFTβ-HA rev (ccccgcagatctctatgcatagtctggtacgtcataagggtatgcatagtctggtacgtcataagggtatgcatagtctggtacgtcataagggtactcgagctcgccgcttctttttgagct), bxrespectively, and ligated into vector pG-EGFPΔLII β (44) (kindly provided by Isabel Roditi, University of Bern, Bern, Switzerland), previously digested with HindIII and BglII. The resulting vectors pG-RFT1ΔLII β and pG-RFT1-HAΔLII β were digested with NotI prior to transfection into Δ*Tbrft1* cells. Clones were obtained by limiting dilution under antibiotic selection using 2 μg/ml puromycin. For the expression of tetracycline-inducible *Tb*RFT1-HA, the gene was PCR-amplified using primers TbRFT1-HA_fwd (tgtagcgggcccatggacttcaaacgacagctg) and TbRFT1-HA_rev (cctcatgcatctagactcgccgcttctttttgagct), digested with ApeI and XbaI, and ligated into equally digested vector pALC14-HA (original vector pALC14 kindly provided by André Schneider, University of Bern), containing a 3× HA tag downstream of the C-terminal restriction site. The resulting vector pALC14-TbRFT1-HA was linearized with NotI prior to transfection into *T. brucei*, strain Lister 427 29-13 procyclic forms. Clones were obtained by limiting dilution under antibiotic selection using 2 μg/ml puromycin.

Immunofluorescence Microscopy of Trypanosomes—2×10^6 cells were harvested at mid-log phase, washed twice in cold PBS (137 mM $NaCl_2$, 2.7 mM KCl, 10 mM Na_2PO_4, 2 mM KH_2PO_4, pH 7.4), and spotted on microscope slides. After adherence, cells were fixed with 4% paraformaldehyde in PBS for 5 min, washed with cold PBS, and permeabilized with 0.2% (w/v) Triton X-100 in PBS for 5 min. Subsequently, cells were blocked with 2% (w/v) bovine serum albumin in PBS prior to incubation with blocking solution containing primary antibodies (mouse monoclonal anti-HA 11, 16B12 (1:200; Enzo Life Sciences; catalog number ENZ-ABS118-0500, lot 04211508), rabbit polyclonal anti-BiP (1:2500) and rabbit polyclonal anti-cathepsin L (1:500) (both kindly provided by J. Bangs, University of Buffalo, Buffalo, NY), and rabbit polyclonal anti-*Tb*GRASP (1:1500; kindly provided by G. Warren, Vienna Biocenter, Vienna, Austria)). Fluorescent secondary antibodies with different excitation and emission maxima were used to visualize *Tb*RFT1-HA separately from BiP, *Tb*GRASP, and cathepsin L, respectively (Alexa Fluor goat anti-mouse 488 (Invitrogen, catalog number A11001, lot 1170048) and goat anti-rabbit 594 (Invitrogen, catalog number A11005, lot 1750828), diluted 1:1000 in blocking solution). Coverslips were mounted on dried slides with VECTASHIELD® containing DAPI (Vector Laboratories) to visualize the nuclei. Pictures were taken with a Leica DM 16000 B inverted microscope combined with a Leica DFC360 FX camera. Image deconvolution (3D deconvolution) and further processing were performed using Leica LAS X software and ImageJ (National Institutes of Health), respectively.

[^{3}H]Etn Labeling of GPI Precursors and GPI-anchored Proteins—For *in vivo* radiolabeling of procyclins, procyclic form trypanosomes were cultured in the presence of [^{3}H]Etn (2 μCi/ml) during 16 h to a density of ~1.5×10^7 cells/ml, as described before (25). Cells were counted, harvested by centrifugation, and washed twice in cold TBS (10 mM Tris-HCl, pH 7.5, 144 mM NaCl). Bulk lipids from up to 2.5×10^8 cells were extracted from the cell pellets using 2 × 10 ml chloroform/methanol (2:1, v/v), and GPI precursors and free GPIs were extracted using 3 × 5 ml of chloroform/methanol/water (10:10:3, v/v/v) (25). GPI-anchored proteins were extracted from the remaining protein pellet using 2 × 1 ml of 9% (v/v) butan-1-ol in water during 2 h on ice, followed by 10 min of centrifugation at 17,000 × *g*. The resulting supernatants were pooled, dried under a stream of nitrogen, and dissolved in electrophoresis sample buffer containing 2.5% (w/v) SDS. Butan-1-ol-insoluble material was further extracted with 0.1% (w/v) Triton X-100 in 20 mM Tris (pH 7.4) for 10 min at 95 °C (25). Radioactivity in the butan-1-ol and Triton X-100 extracts was determined by liquid scintillation counting of small aliquots. For the analysis of [^{3}H]Etn-labeled GPI precursors, all cultures were adjusted to 1.5×10^7 cells/ml prior to incubation with 4 μCi/ml [^{3}H]Etn during 4 h. After washing with TBS and extraction of bulk lipids using 2 × 10 ml chloroform/methanol (2:1, v/v), GPI precursors were extracted by 3 × 5 ml of chloroform/methanol/water (10:10:3, v/v/v). The resulting supernatants were pooled, dried under a stream of nitrogen, and partitioned between 0.5 ml of butan-1-ol and water. After a second extraction of the resulting water phase with 0.5 ml of water-saturated butan-1-ol, butanol phases were pooled and dried using a SpeedVac apparatus. Dry GPI lipids were resuspended in 50 μl of chloroform/methanol/water (10:10:3, v/v/v) and separated by TLC as described below.

Protein Analysis—Proteins from butan-1-ol and Triton X-100 extracts were separated by SDS-PAGE using 12% polyacrylamide gels. [^{3}H]Etn-labeled proteins were analyzed by soaking the fixed gel in Amplify™ for 1 h, drying at 80 °C for 2 h, and exposing to MXBE film at −70 °C. HA-tagged *Tb*RFT1, EP, and GPEET procyclins were analyzed by immunoblotting

onto polyvinylidene difluoride membranes and enhanced chemiluminescence using mouse anti-HA antibody (HA11, diluted 1:3000 in TBS containing 5% skimmed milk powder; Enzo Life Sciences), mouse anti-EP antibody (mouse monoclonal anti-EP 247, diluted 1:1000 in TBS, 5% milk; Cedarlane Labs, Burlington, Ontario Canada; catalog number CLP001A, lot P115), and mouse anti-GPEET 5H3 antibody (diluted 1:5000 in TBS, 5% milk; Cedarlane Labs, lot number 991109 (45)), respectively, followed by HRP-conjugated anti-mouse IgG (diluted 1:5000 in TBS, 5% milk; Dako, Baar, Switzerland). MXBE films were exposed to ECL-activated membranes (SuperSignal West Pico, Pierce-Thermo Fisher) for 30 s to a few minutes.

Mass Spectrometry Analysis—For the analysis of procyclin C-terminal polypeptides, total procyclins were purified by sequential extraction with chloroform/methanol/water (10:10:3, by volume) and 9% (v/v) butan-1-ol as described above. Butan-1-ol extracts were then dried, dephosphorylated with 48% anhydrous hydrofluoric acid for 24 h at 0 °C, hydrolyzed with mild (40 mM) trifluoroacetic acid, and then analyzed by negative-ion MALDI-TOF on an ABI Voyager DE-STR instrument using sinapinic acid as the matrix (12). To determine the total monosaccharide composition of procyclins, samples were mixed with 200 pmol of *scyllo*-inositol (as internal standard) and analyzed by GC-MS as described elsewhere (46).

Enzyme Treatments—For PNGase treatment, parasites were lysed by boiling 10 min at 100 °C in denaturing buffer (0.5% SDS, 40 mM DTT) and incubated with PNGase F (New England Biolabs) according to the manufacturer's instructions in a buffer containing 1% Nonidet P-40 during 1 h at 37 °C. For Pronase treatment, ^{3}H-labeled GPI extracts were dried under a stream of nitrogen, re-dissolved in a buffer containing 20 mM Tris (pH 7.5) and 5 mM $CaCl_2$, and incubated with Pronase (0.3 mg/ml) during 16 h at 37 °C.

Cell-free GPI Glycosylation Analysis—Membranes for cell-free labeling of GPI precursors were collected from trypanosome cultures grown to a density of 10^7 cells/ml by hypotonic lysis in water containing 0.1 mM tosyl-L-lysyl-chloromethane hydrochloride (TLCK) and 1.25 μg/ml leupeptin. Pulse-chase radiolabeling of GPI precursors with [^{3}H]GDP-Man was performed essentially according to the protocol developed by Masterson *et al.* (47) as described by Leal *et al.* (48). If indicated, experiments were performed in the presence of 0.4 mg/ml tunicamycin in the assay buffer to inhibit the formation of dolichol-linked *N*-glycan precursors. In pulse-chase experiments, membranes from 1.5×10^8 cells were labeled with 3 μCi of [^{3}H]GDP-Man and 1 mM UDP-GlcNAc for 8 min at 37 °C, followed by a 75-min chase with 2 mM non-radioactive GDP-Man. For the analysis of GPI galactosylation, 8 mM UDP-Gal was added during the chase with GDP-Man. GPI lipids were extracted as described (47). Butan-1-ol extracts were separated by TLC on Silica Gel 60 plates (Merck Millipore) using chloroform/methanol/water (10:10:3, v/v/v) as solvent system and analyzed using a radioactivity TLC scanner (Berthold Technologies, Regensburg, Switzerland). For autoradiography, TLC plates were treated with EN^{3}HANCE™ spray (Perkin Elmer) prior to exposure to film at −70 °C.

Flow Cytometry—Trypanosomes were grown in the presence or absence of tunicamycin (1 μg/ml) during 10 days. Approximately 1×10^7 parasites were harvested by centrifugation at 4 °C for 10 min at $1500 \times g$ in 15-ml centrifuge tubes, washed twice in ice-cold SDM-79, and resuspended in 200 μl of SDM-79 containing 0.5 mM $MnCl_2$. Concanavalin A-FITC conjugate was added to a final concentration of 1.5 μg/ml. After 1 h of incubation in the dark on ice, the cells were diluted with ice-cold PBS to a volume of 5 ml, pelleted, resuspended in a final volume of 2 ml (final concentration 5×10^6/ml PBS), and passed through a cell-filter cap prior to analysis by FACSCalibur (BD Biosciences). Data were analyzed using flow cytometry software FlowJo.

Author Contributions—P. G. designed, performed, and analyzed the experiments shown in Figs. 1*C* and 3–6 and prepared all figures. A. G. S. generated RFT1 addback-strains and performed the experiment shown in Fig. 1*B*. Y. C. L. and A. A. S. developed the protocol for *in vitro* galactosylation of GPI precursors. A. A. S. designed the scheme in Fig. 1*A* and designed and performed mass spectrometry analyses presented in Fig. 2. P. B. conceived and coordinated the study, and P. B. and P. G. wrote the paper. A. A. S. and A. K. M. provided scientific and experimental advice and critically revised the paper.

Acknowledgments—We thank Luce Farine for generating a T. brucei procyclic form cell line expressing TbEMC3-HA and Jennifer Jelk and Monika Rauch for excellent technical assistance during parts of the study. We also thank the Dundee University Proteomics Facility and Mike Ferguson for generous use of the MALDI Voyager and GC-MS, respectively, and Aitor Casas-Sánchez for the tunicamycin protocol. We thank William White for stimulating discussions.

References

1. Sutton, R. E., and Boothroyd, J. C. (1986) Evidence for *Trans* splicing in trypanosomes. *Cell* **47,** 527–535
2. Blum, B., Bakalara, N., and Simpson, L. (1990) A model for RNA editing in kinetoplastid mitochondria: RNA molecules transcribed from maxicircle DNA provide the edited information. *Cell* **60,** 189–198
3. Cross, G. A. (1977) Antigenic variation in trypanosomes. *Am. J. Trop. Med. Hyg.* **26,** 240–244
4. Ferguson, M. A., Homans, S. W., Dwek, R. A., and Rademacher, T. W. (1988) Glycosyl-phosphatidylinositol moiety that anchors *Trypanosoma brucei* variant surface glycoprotein to the membrane. *Science* **239,** 753–759
5. Ferguson, M. A. J. (1999) The structure, biosynthesis and functions of glycosylphosphatidylinositol anchors, and the contributions of trypanosome research. *J. Cell Sci.* **112,** 2799–2809
6. Allen, G., Gurnett, L. P., and Cross, G. A. M. (1982) Complete amino acid sequence of a variant surface glycoprotein (VSG 117) from *Trypanosoma brucei*. *J. Mol. Biol.* **157,** 527–546
7. Roditi, I., Carrington, M., and Turner, M. (1987) Expression of a polypeptide containing a dipeptide repeat is confined to the insect stage of *Trypanosoma brucei*. *Nature* **325,** 272–274
8. Mowatt, M. R., and Clayton, C. E. (1988) Polymorphism in the procyclic acidic repetitive protein gene family of *Trypanosoma brucei*. *Mol. Cell. Biol.* **8,** 4055–4062
9. Roditi, I., Schwarz, H., Pearson, T. W., Beecroft, R. P., Liu, M. K., Richardson, J. P., Bühring, H.-J., Pleiss, J., Bülow, R., Williams, R. O., and Overath, P. (1989) Procycline gene expression and loss of the variant surface glycoprotein during differentiation of *Trypanosoma brucei*. *J. Cell Biol.* **108,** 737–746
10. Ferguson, M. A. J., Murray, P., Rutherford, H., and McConville, M. J. (1993) A simple purification of procyclic acidic repetitive protein and demonstration of a sialylated glycosyl-phosphatidylinositol membrane anchor. *Biochem. J.* **291,** 51–55

11. Treumann, A., Zitzmann, N., Hülsmeier, A., Prescott, A. R., Almond, A., Sheehan, J., and Ferugson, M. A. J. (1997) Structural characterisation of two forms of procyclic acidic repetitive protein expressed by procyclic forms of *Trypanosoma brucei*. *J. Mol. Biol.* **269,** 529–547
12. Acosta-Serrano, A., Cole, R. N., Mehlert, A., Lee, M. G.-S., Ferguson, M. A. J., and Englund, P. T. (1999) The procyclin repertoire of *Trypanosoma brucei*: identification and structural characterization of the Glu-Pro-rich polypeptides. *J. Biol. Chem.* **274,** 29763–29771
13. Izquierdo, L., Mehlert, A., and Ferguson, M. A. J. (2012) The lipid-linked oligosaccharide donor specificities of *Trypanosoma brucei* oligosaccharyltransferases. *Glycobiology.* **22,** 696–703
14. Acosta-Serrano, A., O'Rear, J., Quellhorst, G., Lee, S. H., Hwa, K.-Y., Krag, S. S., and Englund, P. T. (2004) Defects in the *N*-linked oligosaccharide biosynthetic pathway in a *Trypanosoma brucei* glycosylation mutant. *Eukaryot. Cell* **3,** 255–263
15. Manthri, S., Güther, M. L. S., Izquierdo, L., Acosta-Serrano, A., and Ferguson, M. A. J. (2008) Deletion of the *TbALG3* gene demonstrates site-specific *N*-glycosylation and *N*-glycan processing in *Trypanosoma brucei*. *Glycobiology.* **18,** 367–383
16. Koerte, A., Chong, T., Li, X., Wahane, K., and Cai, M. (1995) Suppression of the yeast mutation *rft1-1* by human p53. *J. Biol. Chem.* **270,** 22556–22564
17. Helenius, J., Ng, D. T. W., Marolda, C. L., Walter, P., Valvano, M. A., and Aebi, M. (2002) Translocation of lipid-linked oligosaccharides across the ER membrane requires Rft1 protein. *Nature* **415,** 447–450
18. Haeuptle, M. A., Pujol, F. M., Neupert, C., Winchester, B., Kastaniotis, A. J., Aebi, M., and Hennet, T. (2008) Human RFT1 deficiency leads to a disorder of *N*-linked glycosylation. *Am. J. Hum. Genet.* **82,** 600–606
19. Sanyal, S., Frank, C. G., and Menon, A. K. (2008) Distinct flippases translocate glycerophospholipids and oligosaccharide diphosphate dolichols across the endoplasmic reticulum. *Biochemistry* **47,** 7937–7946
20. Frank, C. G., Sanyal, S., Rush, J. S., Waechter, C. J., and Menon, A. K. (2008) Does Rft1 flip an *N*-glycan lipid precursor? *Nature* **454,** E3–4; discussion E4–5
21. Rush, J. S., Gao, N., Lehrman, M. A., Matveev, S., and Waechter, C. J. (2009) Suppression of Rft1 expression does not impair the transbilayer movement of $Man_5GlcNAc_2$-P-P-dolichol in sealed microsomes from yeast. *J. Biol. Chem.* **284,** 19835–19842
22. Jelk, J., Gao, N., Serricchio, M., Signorell, A., Schmidt, R. S., Bangs, J. D., Acosta-Serrano, A., Lehrman, M. A., Bütikofer, P., and Menon, A. K. (2013) Glycoprotein biosynthesis in a eukaryote lacking the membrane protein Rft1. *J. Biol. Chem.* **288,** 20616–20623
23. Clayton, C. E., and Mowatt, M. R. (1989) The procyclic acidic repetitive proteins of *Trypanosoma brucei*: purification and post-translational modification. *J. Biol. Chem.* **264,** 15088–15093
24. Hwa, K.-Y., Acosta-Serrano, A., Khoo, K.-H., Pearson, T., and Englund, P. T. (1999) Protein glycosylation mutants of procyclic *Trypanosoma brucei*: defects in the asparagine-glycosylation pathway. *Glycobiology* **9,** 181–190
25. Bütikofer, P., Ruepp, S., Boschung, M., and Roditi, I. (1997) "GPEET" procyclin is the major surface protein of procyclic culture forms of *Trypanosoma brucei* brucei strain 427. *Biochem. J.* **326,** 415–423
26. Vassella, E., Van Den Abbeele, J., Bütikofer, P., Renggli, C. K., Furger, A., Brun, R., and Roditi, I. (2000) A major surface glycoprotein of *Trypanosoma brucei* is expressed transiently during development and can be regulated post-transcriptionally by glycerol or hypoxia. *Genes Dev.* **14,** 615–626
27. Acosta-Serrano, A., Vassella, E., Liniger, M., Kunz Renggli, C., Brun, R., Roditi, I., and Englund, P. T. (2001) The surface coat of procyclic *Trypanosoma brucei*: programmed expression and proteolytic cleavage of procyclin in the tsetse fly. *Proc. Natl. Acad. Sci.* **98,** 1513–1518
28. Ferguson, M. A. J., Low, M. G., and Cross, G. A. (1985) Glycosyl-*sn*-1,2-dimyristylphosphatidylinositol is covalently linked to *Trypanosoma brucei* variant surface glycoprotein. *J. Biol. Chem.* **260,** 14547–14555
29. Field, M. C., Menon, A. K., and Cross, G. A. (1991) A glycosylphosphatidylinositol protein anchor from procyclic stage *Trypanosoma brucei*: lipid structure and biosynthesis. *EMBO J.* **10,** 2731–2739
30. Orlean, P., and Menon, A. K. (2007) Thematic review series: Lipid Post-translational Modifications. GPI anchoring of protein in yeast and mammalian cells, or: how we learned to stop worrying and love glycophospholipids. *J. Lipid Res.* **48,** 993–1011
31. Sanyal, S., and Menon, A. K. (2009) Flipping lipids: why an' what's the reason for? *ACS Chem. Biol.* **4,** 895–909
32. Hong, Y., and Kinoshita, T. (2009) Trypanosome glycosylphosphatidylinositol biosynthesis. *Korean J. Parasitol.* **47,** 197–204
33. Mayor, S., Menon, A. K., and Cross, G. A. M. (1992) Galactose-containing glycosylphosphatidylinositols in *Trypanosoma brucei*. *J. Biol. Chem.* **267,** 754–761
34. Izquierdo, L., Nakanishi, M., Mehlert, A., Machray, G., Barton, G. J., and Ferguson, M. A. J. (2009) Identification of a glycosylphosphatidylinositol anchor-modifying β1-3 *N*-acetylglucosaminyl transferase in *Trypanosoma brucei*. *Mol. Microbiol.* **71,** 478–491
35. Nakanishi, M., Karasudani, M., Shiraishi, T., Hashida, K., Hino, M., Ferguson, M. A. J., and Nomoto, H. (2014) TbGT8 is a bifunctional glycosyltransferase that elaborates *N*-linked glycans on a protein phosphatase AcP115 and a GPI-anchor modifying glycan in *Trypanosoma brucei*. *Parasitol. Int.* **63,** 513–518
36. Izquierdo, L., Acosta-Serrano, A., Mehlert, A., and Ferguson, M. A. (2015) Identification of a glycosylphosphatidylinositol anchor-modifying β1–3 galactosyltransferase in *Trypanosoma brucei*. *Glycobiology.* **25,** 438–447
37. He, C. Y., Ho, H. H., Malsam, J., Chalouni, C., West, C. M., Ullu, E., Toomre, D., and Warren, G. (2004) Golgi duplication in *Trypanosoma brucei*. *J. Cell Biol.* **165,** 313–321
38. Lahiri, S., Chao, J. T., Tavassoli, S., Wong, A. K. O., Choudhary, V., Young, B. P., Loewen, C. J. R., and Prinz, W. A. (2014) A conserved endoplasmic reticulum membrane protein complex (EMC) facilitates phospholipid transfer from the ER to mitochondria. *PLoS Biol.* **12,** e1001969
39. Farine, L., Niemann, M., Schneider, A., and Bütikofer, P. (2015) Phosphatidylethanolamine and phosphatidylcholine biosynthesis by the Kennedy pathway occurs at different sites in *Trypanosoma brucei*. *Sci. Rep.* **5,** 16787
40. Martin, K. L., and Smith, T. K. (2006) Phosphatidylinositol synthesis is essential in bloodstream form *Trypanosoma brucei*. *Biochem. J.* **396,** 287–295
41. Mbawa, Z. R., Gumm, I. D., Shaw, E., and Lonsdale-Eccles, J. D. (1992) Characterisation of a cysteine protease from bloodstream forms of *Trypanosoma congolense*. *Eur. J. Biochem.* **204,** 371–379
42. Liu, L., Xu, Y.-X., Caradonna, K. L., Kruzel, E. K., Burleigh, B. A., Bangs, J. D., and Hirschberg, C. B. (2013) Inhibition of nucleotide sugar transport in *Trypanosoma brucei* alters surface glycosylation. *J. Biol. Chem.* **288,** 10599–10615
43. Izquierdo, L., Schulz, B. L., Rodrigues, J. A., Güther, M. L. S., Procter, J. B., Barton, G. J., Aebi, M., and Ferguson, M. A. J. (2009) Distinct donor and acceptor specificities of *Trypanosoma brucei* oligosaccharyltransferases. *EMBO J.* **28,** 2650–2661
44. Furger, A., Schürch, N., Kurath, U., and Roditi, I. (1997) Elements in the 3′ untranslated region of procyclin mRNA regulate expression in insect forms of *Trypanosoma brucei* by modulating RNA stability and translation. *Mol. Cell Biol.* **17,** 4372–4380
45. Bütikofer, P., Vassella, E., Ruepp, S., Boschung, M., Civenni, G., Seebeck, T., Hemphill, A., Mookherjee, N., Pearson, T. W., and Roditi, I. (1999) Phosphorylation of a major GPI-anchored surface protein of *Trypanosoma brucei* during transport to the plasma membrane. *J. Cell Sci.* **112,** 1785–1795
46. Ferguson, M. A. J. (1993) *Glycobiology: A Practical Approach* (Fukuda, M., and Kobata, A. eds), pp. 349–383, Oxford University Press, Oxford
47. Masterson, W. J., Doering, T. L., Hart, G. W., and Englund, P. T. (1989) A novel pathway for glycan assembly: biosynthesis of the glycosyl-phosphatidylinositol anchor of the trypanosome variant surface glycoprotein. *Cell* **56,** 793–800
48. Leal, S., Acosta-Serrano, A., Morris, J., and Cross, G. A. M. (2004) Transposon mutagenesis of *Trypanosoma brucei* identifies glycosylation mutants resistant to concanavalin A. *J. Biol. Chem.* **279,** 28979–28988
49. Hall, B. S., Pal, A., Goulding, D., Acosta-Serrano, A., and Field, M. C. (2005) *Trypanosoma brucei*: TbRAB4 regulates membrane recycling and expression of surface proteins in procyclic forms. *Exp. Parasitol.* **111,** 160–171
50. Field, M. C., Menon, A. K., and Cross, G. A. M. (1991) Developmental variation of glycosylphosphatidylinositol membrane anchors in *Trypanosoma brucei*. *J. Biol. Chem.* **266,** 8392–8400

RFT1 Protein Affects Glycosylphosphatidylinositol (GPI) Anchor Glycosylation

Petra Gottier, Amaia Gonzalez-Salgado, Anant K. Menon, Yuk-Chien Liu, Alvaro Acosta-Serrano and Peter Bütikofer

J. Biol. Chem. 2017, 292:1103-1111.
doi: 10.1074/jbc.M116.758367 originally published online December 7, 2016
